An Advanced Ensemble of Deep Learning Models for Breast Cancer Segmentation and Classification with Two-Tier Optimization Algorithms

M. Sreevani
Department of Computer Science, St. Peter's Institute of Higher Education and Research, Avadi, Tamil Nadu, India | Department of CSE, Vemu Institute of Technology, Chittoor, Andhra Pradesh, India
vani.cse183@gmail.com (corresponding author)

R. Latha
Department of Computer Applications, St. Peter's Institute of Higher Education and Research, Avadi, Tamil Nadu, India
latharamavel1212@gmail.com

Received: 11 June 2025 | Revised: 11 July 2025 | Accepted: 16 July 2025

 DOI: https://doi.org/10.48084/etasr.12682

ABSTRACT

Breast Cancer (BC) is one of the most common cancers among women. Routine mammography is substantial because asymptomatic BC does not show early signs, making early detection difficult. Automated methods, including Deep Learning (DL) models, have gained significant attention for analyzing mammographic images and enhancing diagnostic accuracy. Successful AI training for these medical tasks depends on large datasets with accurately annotated lesion locations. This study proposes an Advanced Ensemble Deep Learning Model for Breast Cancer Segmentation and Classification with a Two-Tier Optimization (AEDL-BCSCT2O) approach to segment and classify BC using advanced DL and optimization techniques. The model initially applies Adaptive Bilateral Filtering (ABF) for noise removal and CLAHE for contrast enhancement to improve image quality. The DeepLabV3+ segmentation method is enhanced through parameter optimization using the Lemur Optimizer (LO). The NASNetMobile model is utilized for feature extraction. An ensemble of Deep Belief Network (DBN), Graph Convolutional Network (GCN), and Sparse Stacked Autoencoder (SSAE) models is used for improved classification. Finally, the Osprey Optimization Algorithm (OOA) approach is utilized for tuning. The validation results show that the AEDL-BCSCT2O method achieves 99.76% accuracy, outperforming existing models.

Keywords-ensemble deep learning; breast cancer; two-tier optimization; feature extraction; image preprocessing

I. INTRODUCTION

Among women, BC is a prevalent cancer, with lung cancer second [1]. BC can develop from any breast tissue, cell, or gland, most commonly originating in the milk-producing ducts or lobules [2]. If left undetected, cancer cells can spread to other parts of the body. BC is classified primarily into benign (non-cancerous) and malignant (cancerous) [3, 4]. Malignant cells proliferate at a higher rate by rapidly initiating division, as both benign and malignant cells exhibit abnormal structures and appearances, presenting a complex challenge for physical examination of microscopic images [5]. The precise diagnosis and early detection of BC are the main factors in improving the analysis and the survival rate of patients with BC [6]. The composite nature of BC, with its varied treatment responses and subdivisions, underscores the need for individualized treatment approaches [7]. Advances in imaging techniques, such as digital radiography, mammography, MRI, and CT, have greatly improved cancer diagnosis and treatment [8]. This technology requires crucial medical image acquisition, examined by radiologists, to play a vital role in diagnostics [9]. Mammography is the key for early detection of BC, and digital advances reduce risks. DL improves biomedical results by effectively modeling features [10].

This study presents an Advanced Ensemble Deep Learning Model for Breast Cancer Segmentation and Classification with a Two-Tier Optimization (AEDL-BCSCT2O) approach. The aim is to segment and classify BC using advanced DL and optimization techniques. The model initially applies Adaptive Bilateral Filtering (ABF) for noise removal and CLAHE for contrast enhancement to improve image quality. The

DeepLabV3+ segmentation method is enhanced through parameter optimization using the Lemur Optimizer (LO). Then, the NASNetMobile model is utilized for feature extraction. Then, an ensemble of Deep Belief Network (DBN), Graph Convolutional Network (GCN), and Sparse Stacked Autoencoder (SSAE) models is used for improved classification. Finally, the Osprey Optimization Algorithm (OOA) approach is utilized for tuning. Simulations were performed on a benchmark dataset. The contributions of this approach are as follows.

- The model applies ABF and CLAHE to remove noise and enhance contrast, improve input image quality, enhance analysis and classification, and improve model accuracy and reliability.
- DeepLabV3+ segmentation is enhanced by optimizing parameters with LO, resulting in improved segmentation accuracy and performance.
- The NASNetMobile model is utilized for effective feature extraction, and ensemble models are tuned with OOA to improve classification accuracy. This integration improves the overall performance and robustness of the model.
- The integration of advanced preprocessing, optimized segmentation, deep feature extraction, and ensemble classification, tuned by OOA, presents a robust framework for accurate image-based diagnosis. This incorporation improves both precision and reliability, addressing key challenges by enhancing feature representation and optimizing performance.

II. LITERATURE WORKS

In [11], an Ensemble of Deep Convolutional Neural Networks (EDCNN) method was presented, which incorporated the strengths of the Xception and MobileNet methods. In [12], an automated method was introduced, employing two DL structures, UNet and SegNet, and the three-time-point (3TP) approach for segmentation. In [13], a novel DL-based approach, named Deep WSI-Stroma, was introduced. In [14], a BC Detection method was presented, which is a unified CAD method that uses DL-based YOLO to detect abnormalities, U-Net to segment masses, and a deep CNN to perform classification. In [15], an optimized CNN ensemble integrated EfficientNet, AlexNet, ResNet, and DenseNet to improve the accuracy of early BC diagnosis. In [16], DL methods were integrated using stacking ensemble techniques, with CNN as meta-predictor. In [17], a DeepLabV3Plus model used a ResNet50 encoder and improved Atrous separable convolutions. In [18], improved BC classification was achieved by integrating a CNN and a Long Short-Term Memory (LSTM) model. In [19], BC classification was improved by incorporating pre-trained DenseNet-121 and EfficientNet-B5 models with Support Vector Machine (SVM) classification, optimized using a metaheuristic algorithm.

Despite advances in EDCNN, DL segmentation, and ensemble methods, many models encounter limitations with limited generalization across diverse datasets and often require high computational resources. Some models lack integration of temporal dependencies or fail to optimize hyperparameters effectively. A research gap also exists in the development of lightweight and scalable models that maintain high accuracy while efficiently handling diverse BC image types and optimizing feature extraction and classification processes.

III. PROPOSED METHOD

This paper presents a novel AEDL-BCSCT2O method, comprising various processes, such as image preprocessing, segmentation, feature extraction, classification, and tuning. Figure 1 shows its working flow.

A. Dataset Description

The utilized dataset is sourced from Kaggle [20] and comprises 3,758 samples classified into two classes: benign and malignant. Table I shows the class distribution of the dataset.

TABLE I. DATASET DESCRIPTION

Class	Number of Samples
Benign	2043
Malignant	1715
Overall samples	**3758**

B. Image Preprocessing

Initially, the AEDL-BCSCT2O approach employs a dual-phase preprocessing, noise elimination using ABF and contrast enhancement using CLAHE, to ensure improved input image quality [21-22]. This dual-phase effectively removes noise while preserving crucial image details, unlike conventional filters that may blur edges. ABF mitigates noise without compromising texture, and CLAHE enhances local contrast, improving the visibility of features. This integration ensures higher image quality, which is significant for accurate downstream analysis and classification compared to simpler or single-step methods. ABF enhances image quality by reducing noise through spatial-intensity averaging while preserving tumor edges, aiding precise segmentation and classification. For contrast enhancement, CLAHE divides images into tiles, applies histogram equalization with clipping, and merges tiles using bilinear interpolation to improve mass visibility.

C. Segmentation Using DeepLabV3+ Architecture

The AEDL-BCSCT2O model utilizes the DeepLabV3+ architecture for the segmentation process and is further enhanced with parameter optimization using LO [23]. This model is chosen for its advanced capability to capture multiscale contextual data through Atrous Spatial Pyramid Pooling (ASPP), enabling precise segmentation of complex image structures. These methods present enhanced accuracy and boundary delineation, and their encoder-decoder design balances detailed feature extraction and spatial resolution, making it more effective than simpler segmentation models. This is a progressive semantical segmentation approach that works above an encoding-decoding architecture. The model's encoder utilizes the original ASPP with five parallel branches to extract spectral, textural, and spatial features, capturing key contextual information for accurate segmentation. A global average pooling layer further enhances the technique's ability to comprehend the overall image content.

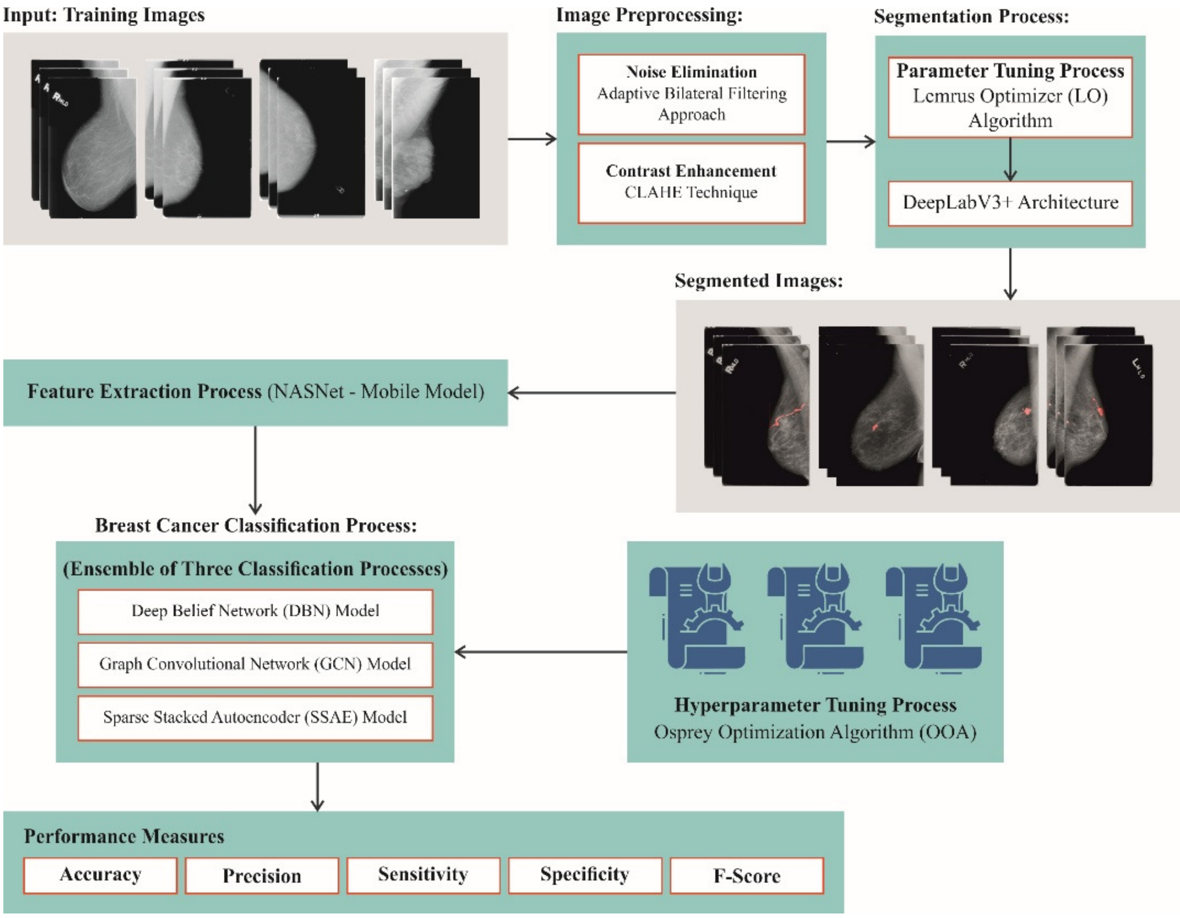

Fig. 1. Workflow of the AEDL-BCSCT2O model.

In the decoding stage, features are up-sampled four times and merged with lower-level features to produce high-resolution maps for accurate erosion detection [24]. The DeepLabV3+ model is optimized using the LO algorithm, inspired by lemurs' leaping and hopping behaviors. To initialize the method, the population of the lemur is randomly positioned inside the variable boundaries, as stated by:

$$L_i^j = rand \times \left(ub_j - lb_j\right) + lb_j,$$
$$\forall i \in (1,2,\ldots,n), \forall j \in (1,2,\ldots,d) \quad (1)$$

where $rand$ denotes a randomly generated number in the interval of (0-1), and ub and lb depict the lower and upper boundaries. Then, the fitness of all lemurs is evaluated using an objective function, establishing the present global best ($gbest$) and the best of its adjacent neighbours ($nbest$). Throughout this exploration stage, mirroring the behaviour of leaping, it performs longer jumps based on:

$$L_{i+1}^j = L_i^j + abs\left(L_i^j - gbest^j\right) \times (rand - 0.5) \times 2\,,$$
$$\text{if } rand \geq FRR \quad (2)$$

During this exploitation stage resembling dance-hopping, it interacts with neighbouring lemurs as per:

$$L_{i+1}^j = L_i^j + abs\left(L_i^j - nbest^j\right) \times (rand - 0.5) \times 2,$$
$$\text{if } rand < FRR \quad (3)$$

The dynamical modification of the risk parameter FRR, utilizing (4), guarantees adaptabilities in the optimizer procedure:

$$PRR = HRR - Crnt_{Iter} \times \left(\frac{(HRR-LRR)}{\text{Max\_}Iter}\right) \quad (4)$$

Here, HRR and LRR characterize constant predefined values, $Crnt\_Iter$ signifies the present iteration, and $\text{Max\_}Iter$ denotes a maximal number of iterations.

D. Feature Extraction using NASNetMobile Model

Next, the NASNetMobile model is employed to extract relevant features from images [23]. This method is chosen for its efficiency and high-quality feature extraction with fewer parameters. Its optimized architecture delivers robust features while keeping computational costs low, making it ideal for resource-limited settings. This NAS-designed model utilizes reduction and normal cells to capture detailed, complex features, striking a balance between accuracy and efficiency through separable convolutions and regularization and making it effective for detecting subtle shape and texture changes. The NASNetMobile cell processes input X through a mapping function $F(X, W_i)$, which includes key operations such as separable convolution, batch normalization, ReLU activation, and pooling. The output Y is attained by adding the original input X to the mapped features, expressed as:

$$Y = F(X, W_i) + X \quad (5)$$

where W_i represents the learnable parameters, and the addition is performed element-wise, enabling the model to learn residual representations efficiently.

E. Classification Using Ensemble Models

An ensemble of three classification processes is employed, involving a DBN model, a GCN classifier, and an SSAE approach. The ensemble model is chosen for its ability to capture diverse aspects of the data. DBN excels at learning hierarchical features, GCN effectively models relational information in graph structures, and SSAE provides robust feature learning through sparse representations. Integrating these models improves overall classification accuracy and noise resistance, outperforming single classifiers.

1) DBN Model

DBN is a DL model integrating unsupervised RBM-based pretraining and supervised fine-tuning [25]. It efficiently learns hierarchical features and performs well even on smaller datasets through greedy layer-wise training. The RBM-based weights are upgraded using greedy layer-wise training. Every RBM contains a connection among the adjacent n^{th} and $(n+1)^{th}$ layers. The b_n and c_n for h_n and h_{n+1} are denoted as bias parameters:

$$E(h_n, h_{n+1}) = -h_{n+1}Wh_n - b_nh_n - c_nh_{n+1} \quad (6)$$

$$P(h_n, h_{n+1}) = \frac{e^{-E(h_n,h_{n+1})}}{\sum e^{-E(h_n,h_{n+1})}} \quad (7)$$

$P(h_n, h_{n+1})$ denotes the joint distribution of RBM, and $E(h_n, h_{n+1})$ indicates an energy function among the n^{th} and $(n+1)^{th}$ layers. DBN extracts high-level features using multiple hidden layers with RBM-based representations.

2) GCN Classifier

GCNs are effective for learning from irregular data structures using graph-based operations [26]. Given a feature matrix X, an adjacency matrix A, and a degree matrix D, the standardized forward propagation for the first GCN layer is:

$$L^{[1]} = \sigma\left(D^{-\frac{1}{2}}AD^{-\frac{1}{2}}L^{[0]}W^{[0]}\right) \quad (8)$$

where σ is the ReLU activation function, $W^{[0]}$ is the trainable weight matrix, and $D^{-\frac{1}{2}}AD^{-\frac{1}{2}}$ normalizes the graph to stabilize training. The model learns each node's features from its neighbourhood, and cross-entropy loss is utilized for training on labelled samples.

3) SSAE Method

An Autoencoder (AE) consists of an encoding portion and a decoding portion, which is an ANN trained in unsupervised learning [27]. An AE is an unsupervised neural network with input, hidden, and decoding layers that learns efficient data representations. Its loss function combines MSE, L2 regularization, and a sparsity penalty defined as:

$$E = MSE + (\lambda \times L2Regularization\ Term) + (\beta \times SparsityRegularization\ Term) \quad (9)$$

where λ and β are coefficients. The sparsity penalty uses Kullback-Leibler (KL) divergence:

$$KL(\rho \| \hat{\rho}_j) = (\rho)log\left(\frac{\rho}{\hat{\rho}_j}\right) + (1-\rho)log\left(\frac{1-\rho}{1-\hat{\rho}_j}\right) \quad (10)$$

Stacking multiple sparse AEs forms an SSAE for deeper feature extraction.

F. Hyperparameter Tuning Using OOA

Finally, the parameters of the three ensemble models are tuned using the OOA approach [28], chosen for its effective balance of exploration and exploitation, enabling efficient global search and faster convergence. This model reduces the risk of getting trapped in local optima and is less sensitive to initial parameters, leading to more reliable tuning and improved performance. The metaheuristic model replicates osprey hunting behavior to solve global optimization, balancing exploration for broad search and exploitation for solution refinement. It starts with random initialization of each osprey's position within variable bounds:

$$x_{i,j} = b_{1,j} + r_{i,j}(b_{u,j} - b_{1,j}) \quad (11)$$

where $x_{i,j}$ is the position of the i^{th} osprey in the j^{th} dimension, $b_{1,j}$ and $b_{u,j}$ are the lower and upper bounds, and $r_{i,j} \in [0, 1]$.

In the exploration phase, ospreys update their positions based on prey (better solutions):

$$x_{i,j}^1 = x_{i,j} + r_{i,j}(P_{i,j}^S - l_{i,j} \cdot x_{i,j}) \quad (12)$$

In the exploitation phase, after identifying prey, they refine their positions using a similar update rule:

$$x_{i,j}^2 = x_{i,j} + r_{i,j}(P_{i,j}^S - l_{i,j} \cdot x_{i,j}) \quad (13)$$

These phases enable OOA to avoid local optima and ensure faster, stable convergence. The WGO method creates a fitness function based on the reduction of classifier error rate to improve classification:

$$fitness(x_i) = ClassifierErrorRate(x_i) = \frac{Number\ of\ misclassified\ samples}{Overall\ samples} \times 100 \quad (14)$$

IV. PERFORMANCE ANALYSIS

This section presents the performance evaluation of the AEDL-BCSCT2O method, demonstrating its efficiency through various metrics and comparative analyses. The model was run on Python 3.6.5 with an Intel i5-8600k CPU, 4GB GPU, 16GB RAM, 250GB SSD, and 1TB HDD, using a learning rate of 0.01, ReLU activation, 50 epochs, 0.5 dropout, and a batch size of 5.

Figure 2 shows the classification output of the AEDL-BCSCT2O model. Figures 2(a, b) show confusion matrices at

70:30 TRPH/TSPH. Figures 2(c, d) present the PR and ROC curves, indicating strong performance across classes.

Table II presents a comparative analysis of the AEDL-BCSCT2O method over existing models [29-32], including their Computational Time (CT) results. The analysis exhibits that models such as SVM, Logistic Regression (LR), Naïve Bayes (NB), EfficientNet-B3-ImageNet, AlexNet-SVM, AlexNet-DBN, DenseNet201-ChexNet, VGG+TL, ResNet50, and NER SVM attained relatively lower performance metrics. Specifically, these models exhibited varied $accu_y$, $prec_n$, $reca_l$, and $F1_{score}$ values, accompanied by higher CT values, ranging from 11.34 to 19.94 s. In contrast, the AEDL-BCSCT2O approach demonstrated better outputs, achieving the highest $accu_y$, $prec_n$, $reca_l$, and $F1_{score}$ of 99.76%, 99.71%, 99.76%, and 99.73%, respectively, while also recording the lowest CT of 8.85 s, thereby illustrating both enhanced performance and efficiency.

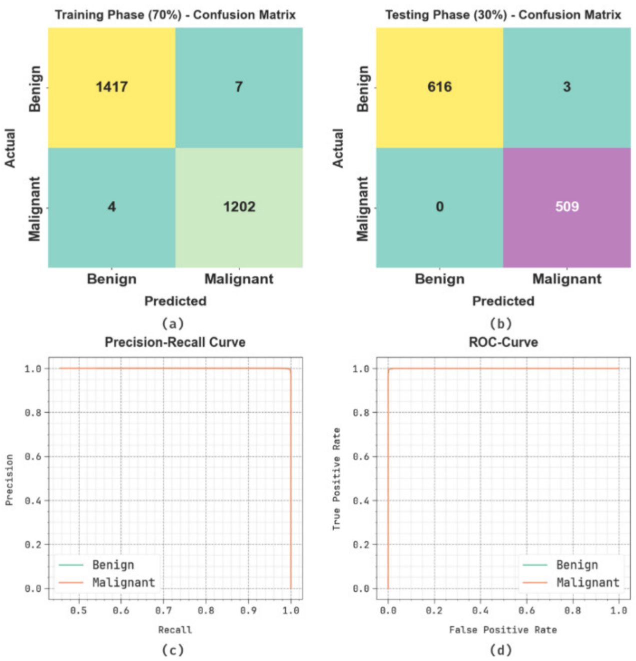

Fig. 2. Classifier outcomes of confusion matrices (a, b), and PR and ROC curves (c, d).

TABLE II. COMPARISON OF AEDL-BCSCT2O APPROACH WITH EXISTING CLASSIFIERS [29-32]

Approaches	$Accu_y$	$Prec_n$	$Reca_l$	$F1_{score}$	CT
SVM	93.81	96.97	94.06	92.15	11.34
LR	96.41	98.05	97.52	98.60	19.94
NB Model	94.73	98.60	96.90	91.99	19.60
EfficientNet-B3-ImageNet	89.00	92.51	98.22	92.86	19.50
AlexNet-SVM	91.00	95.64	95.65	97.22	19.22
AlexNet-DBN	96.32	97.58	96.20	97.71	15.08
DenseNet201-ChexNet	98.60	98.36	92.80	98.70	14.62
VGG+TL	92.49	96.47	92.33	94.01	16.25
ResNet50	98.00	94.24	93.09	93.53	15.10
NER SVM Model	96.73	92.55	97.26	97.73	16.49
AEDL-BCSCT2O	99.76	99.71	99.76	99.73	8.85

V. CONCLUSION

This paper presents a novel AEDL-BCSCT2O method. The model initially applied ABF for noise removal and CLAHE for contrast enhancement to improve image quality. The DeepLabV3+ segmentation method was enhanced by parameter optimization using LO. Then, the NASNetMobile model was utilized for feature extraction. In addition, an ensemble of DBN, GCN, and SSAE models was used for improved classification. Finally, the OOA model was used for tuning. The validation results show that the AEDL-BCSCT2O method achieves 99.76% accuracy, outperforming existing models. The limitations comprise the reliance on limited dataset diversity and the requirement for improved generalization across varied populations. Further research may explore integrating multi-modal data and improving model interpretability for broader clinical application.

REFERENCES

[1] S. Sakib, N. Yasmin, A. K. Tanzeem, F. Shorna, K. Md. Hasib, and S. B. Alam, "Breast Cancer Detection and Classification: A Comparative Analysis Using Machine Learning Algorithms," in *Proceedings of Third International Conference on Communication, Computing and Electronics Systems*, 2022, pp. 703–717, https://doi.org/10.1007/978-981-16-8862-1_46.

[2] X. Wang *et al.*, "Intelligent Hybrid Deep Learning Model for Breast Cancer Detection," *Electronics*, vol. 11, no. 17, Jan. 2022, Art. no. 2767, https://doi.org/10.3390/electronics11172767.

[3] G. Hamed, M. A. E. R. Marey, S. E. S. Amin, and M. F. Tolba, "Deep Learning in Breast Cancer Detection and Classification," in *Proceedings of the International Conference on Artificial Intelligence and Computer Vision (AICV2020)12682*, 2020, pp. 322–333, https://doi.org/10.1007/978-3-030-44289-7_30.

[4] N. M. ud din, R. A. Dar, M. Rasool, and A. Assad, "Breast cancer detection using deep learning: Datasets, methods, and challenges ahead," *Computers in Biology and Medicine*, vol. 149, Oct. 2022, Art. no. 106073, https://doi.org/10.1016/j.compbiomed.2022.106073.

[5] M. Kumar, S. Singhal, S. Shekhar, B. Sharma, and G. Srivastava, "Optimized Stacking Ensemble Learning Model for Breast Cancer Detection and Classification Using Machine Learning," *Sustainability*, vol. 14, no. 21, Jan. 2022, Art. no. 13998, https://doi.org/10.3390/su142113998.

[6] B. S. Abunasser, M. R. J. AL-Hiealy, I. S. Zaqout, and S. S. Abu-Naser, "Breast cancer detection and classification using deep learning Xception algorithm," *International Journal of Advanced Computer Science and Applications*, vol. 13, no. 7, 2022.

[7] A. Saber, M. Sakr, O. M. Abo-Seida, A. Keshk, and H. Chen, "A Novel Deep-Learning Model for Automatic Detection and Classification of Breast Cancer Using the Transfer-Learning Technique," *IEEE Access*, vol. 9, pp. 71194–71209, 2021, https://doi.org/10.1109/ACCESS.2021.3079204.

[8] T. N. Nguyen, T. T. Nguyen, T. H. Nguyen, and B. V. Ngo, "A Robust Approach for Breast Cancer Classification from DICOM Images," *Engineering, Technology & Applied Science Research*, vol. 15, no. 3, pp. 23499–23505, Jun. 2025, https://doi.org/10.48084/etasr.10931.

[9] A. Naz, H. Khan, I. Ud Din, A. Ali, and M. Husain, "An Efficient Optimization System for Early Breast Cancer Diagnosis based on Internet of Medical Things and Deep Learning," *Engineering, Technology & Applied Science Research*, vol. 14, no. 4, pp. 15957–15962, Aug. 2024, https://doi.org/10.48084/etasr.8080.

[10] O. I. Ramadan *et al.*, "Enhancing Breast Cancer Classification based on BPSO Feature Selection and Machine Learning Techniques," *Engineering, Technology & Applied Science Research*, vol. 15, no. 3, pp. 23907–23916, Jun. 2025, https://doi.org/10.48084/etasr.10900.

[11] M. R. Islam *et al.*, "Enhancing breast cancer segmentation and classification: An Ensemble Deep Convolutional Neural Network and U-

net approach on ultrasound images," *Machine Learning with Applications*, vol. 16, Jun. 2024, Art. no. 100555, https://doi.org/10.1016/j.mlwa.2024.100555.

[12] E. D. Carvalho, O. P. da Silva Neto, and A. O. de Carvalho Filho, "Deep learning-based tumor segmentation and classification in breast MRI with 3TP method," *Biomedical Signal Processing and Control*, vol. 93, Jul. 2024, Art. no. 106199, https://doi.org/10.1016/j.bspc.2024.106199.

[13] T. Huang, H. Yin, and X. Huang, "Deep learning and multiscale analysis for epithelial-mesenchyme segmentation and classification in breast cancer histological images," *Signal, Image and Video Processing*, vol. 18, no. 11, pp. 7741–7754, Nov. 2024, https://doi.org/10.1007/s11760-024-03424-6.

[14] M. Arfi, S. C. Yadav, and S. L. Tripathi, "An integrated computer-aided diagnosis BCanD model for detection, segmentation and classification of breast cancer," *Engineering Research Express*, vol. 6, no. 3, Jun. 2024, Art. no. 035240, https://doi.org/10.1088/2631-8695/ad780e.

[15] D. Shah, M. A. U. Khan, M. Abrar, and M. Tahir, "Optimizing Breast Cancer Detection With an Ensemble Deep Learning Approach," *International Journal of Intelligent Systems*, vol. 2024, no. 1, 2024, Art. no. 5564649, https://doi.org/10.1155/2024/5564649.

[16] F. Gurcan, "Enhancing breast cancer prediction through stacking ensemble and deep learning integration," *PeerJ Computer Science*, vol. 11, Feb. 2025, Art. no. e2461, https://doi.org/10.7717/peerj-cs.2461.

[17] S. Lee, Y. Zhao, and W. Choi, "High-rate emphasized DeepLabV3Plus for Semantic Segmentation of Breast Cancer-related Hematoxylin and Eosin-stained Images," in *2024 46th Annual International Conference of the IEEE Engineering in Medicine and Biology Society (EMBC)*, Orlando, FL, USA, Jul. 2024, pp. 1–4, https://doi.org/10.1109/embc53108.2024.10782325.

[18] M. Kaddes, Y. M. Ayid, A. M. Elshewey, and Y. Fouad, "Breast cancer classification based on hybrid CNN with LSTM model," *Scientific Reports*, vol. 15, no. 1, Feb. 2025, Art. no. 4409, https://doi.org/10.1038/s41598-025-88459-6.

[19] A. Saber, S. Elbedwehy, W. A. Awad, and E. Hassan, "An optimized ensemble model based on meta-heuristic algorithms for effective detection and classification of breast tumors," *Neural Computing and Applications*, vol. 37, no. 6, pp. 4881–4894, Feb. 2025, https://doi.org/10.1007/s00521-024-10719-9.

[20] "CBIS-DDSM: Breast Cancer Image Dataset." Kaggle, [Online]. Available: https://www.kaggle.com/datasets/awsaf49/cbis-ddsm-breast-cancer-image-dataset.

[21] S. Mudrakola and N. Hegde, "Removal of noise on mammogram breast images using filtering methods," *Concurrency and Computation: Practice and Experience*, vol. 35, no. 1, 2023, Art. no. e7444, https://doi.org/10.1002/cpe.7444.

[22] Z. Jiang *et al.*, "Evaluating Recalibrating AI Models for Breast Cancer Diagnosis in a New Context: Insights from Transfer Learning, Image Enhancement and High-Quality Training Data Integration," *Cancers*, vol. 16, no. 2, Jan. 2024, Art. no. 322, https://doi.org/10.3390/cancers16020322.

[23] A. A. Abd El-Aziz, M. A. Mahmood, and S. Abd El-Ghany, "Advanced Deep Learning Fusion Model for Early Multi-Classification of Lung and Colon Cancer Using Histopathological Images," *Diagnostics*, vol. 14, no. 20, Jan. 2024, Art. no. 2274, https://doi.org/10.3390/diagnostics14202274.

[24] M. A. Al-Betar, A. K. Abasi, Z. A. A. Alyasseri, S. Fraihat, and R. F. Mohammed, "A Communication-Efficient Federated Learning Framework for Sustainable Development Using Lemurs Optimizer," *Algorithms*, vol. 17, no. 4, Apr. 2024, Art. no. 160, https://doi.org/10.3390/a17040160.

[25] G. Altan, "Breast cancer diagnosis using deep belief networks on ROI images," *Pamukkale Üniversitesi Mühendislik Bilimleri Dergisi*, vol. 28, no. 2, pp. 286–291, Apr. 2022.

[26] S. Palmal, N. Arya, S. Saha, and S. Tripathy, "Breast cancer survival prognosis using the graph convolutional network with Choquet fuzzy integral," *Scientific Reports*, vol. 13, no. 1, Sep. 2023, Art. no. 14757, https://doi.org/10.1038/s41598-023-40341-z.

[27] V. J. Kadam, S. M. Jadhav, and K. Vijayakumar, "Breast Cancer Diagnosis Using Feature Ensemble Learning Based on Stacked Sparse Autoencoders and Softmax Regression," *Journal of Medical Systems*, vol. 43, no. 8, Jul. 2019, Art. no. 263, https://doi.org/10.1007/s10916-019-1397-z.

[28] D. Zheng, Y. Zhang, X. Guo, Y. Ning, and R. Wei, "Research on the remaining useful life prediction method for lithium-ion batteries based on feature engineering and CNN-BiGRU-AM model," *Ionics*, vol. 31, no. 6, pp. 5717–5736, Jun. 2025, https://doi.org/10.1007/s11581-025-06293-2.

[29] V. Jaiswal, P. Saurabh, U. K. Lilhore, M. Pathak, S. Simaiya, and S. Dalal, "A breast cancer risk predication and classification model with ensemble learning and big data fusion," *Decision Analytics Journal*, vol. 8, Sep. 2023, Art. no. 100298, https://doi.org/10.1016/j.dajour.2023.100298.

[30] R. Qasrawi *et al.*, "Hybrid ensemble deep learning model for advancing breast cancer detection and classification in clinical applications," *Heliyon*, vol. 10, no. 19, Oct. 2024, https://doi.org/10.1016/j.heliyon.2024.e38374.

[31] Z. Liu, J. Peng, X. Guo, S. Chen, and L. Liu, "Breast cancer classification method based on improved VGG16 using mammography images," *Journal of Radiation Research and Applied Sciences*, vol. 17, no. 2, Jun. 2024, Art. no. 100885, https://doi.org/10.1016/j.jrras.2024.100885.

[32] S. Arooj *et al.*, "Data Fusion Architecture Empowered with Deep Learning for Breast Cancer Classification," *Computers, Materials & Continua*, vol. 77, no. 3, pp. 2813–2831, 2023, https://doi.org/10.32604/cmc.2023.043013.